Hindawi Publishing Corporation
International Journal of Photoenergy
Volume 2008, Article ID 150682, 8 pages
doi:10.1155/2008/150682

Research Article

Two-Dimensional Free Energy Surfaces for Electron Transfer Reactions in Solution

Shigeo Murata,[1] Maged El-Kemary,[2] and M. Tachiya[1]

[1] *National Institute of Advanced Industrial Science and Technology (AIST), AIST Tsukuba Central 5, 1-1-1 Higashi, Tsukuba 305-8565, Japan*
[2] *Chemistry Department, Faculty of Education, Kafr ElSheikh University, Kafr ElSheikh 33516, Egypt*

Correspondence should be addressed to Shigeo Murata, shigeo.murata@aist.go.jp

Received 2 May 2008; Revised 18 June 2008; Accepted 18 August 2008

Recommended by Mohamed Sabry Abdel-Mottaleb

Change in intermolecular distance between electron donor (D) and acceptor (A) can induce intermolecular electron transfer (ET) even in nonpolar solvent, where solvent orientational polarization is absent. This was shown by making simple calculations of the energies of the initial and final states of ET. In the case of polar solvent, the free energies are functions of both D-A distance and solvent orientational polarization. On the basis of 2-dimensional free energy surfaces, the relation of Marcus ET and exciplex formation is discussed. The transient effect in fluorescence quenching was measured for several D-A pairs in a nonpolar solvent. The results were analyzed by assuming a distance dependence of the ET rate that is consistent with the above model.

1. INTRODUCTION

Electron transfer (ET) reactions have been studied extensively for many years. Fluorescence quenching is often used to study ET reactions involving excited molecules. Two types of ET reactions have been identified in fluorescence quenching: full ET from the electron donor (D) to the acceptor (A) yielding D^+ and A^- radical ions, and partial ET yielding a fluorescent complex [1]. The former mainly occurs in polar environments, and is less important in less polar environments. This process is attributed to Marcus nonadiabatic ET. The latter, on the other hand, mainly occurs in nonpolar and weakly polar environments, and is less important in more polar environments. This process is attributed to the formation of the excited-state charge-transfer complex (the exciplex). This result is supported by many other results for various D-A systems [2–4]. It was shown later [5–8] that the mechanism depends not only on the solvent polarity but also on ΔG of the reaction: quenching by exciplex formation also occurs in polar solvents for D-A pairs with smaller $-\Delta G$, the degree of charge transfer of the exciplex changes in a wide range (from ~0 to >90%) depending on ΔG and solvent polarity. These results are based on spectroscopic and dipole moment measurements.

In Marcus theory, ET occurs when the free energies of the initial and final states of ET coincide as a result of change of solvent coordinate (coordinate representing the solvent orientational polarization). The solvent orientational polarization coordinate is relevant to this type of ET. On the other hand, the coordinate relevant to exciplex formation is not clear. Exciplex formation can occur efficiently even in nonpolar solvents, where Marcus ET does not occur because of the lack of solvent orientational polarization. This indicates that some other coordinate is relevant to exciplex formation in nonpolar solvents.

In previous papers [9–13], we reported fluorescence quenching by ET between cyanoanthracenes (A) in a donor solvent. By femtosecond fluorescence upconversion experiments [12, 13], we found that the two processes, quenching of acceptor fluorescence and riseup of exciplex fluorescence, have the same time constants (~200 femtoseconds) and occur without delay. This implies that the exciplex is directly formed upon fluorescence quenching, that is, there is no intermediate process between them. Based on this observation, we proposed a mechanism of exciplex formation. According to this mechanism, the exciplex is formed as a result of mixing of the DA^* and D^+A^- states, and the exciplex state is reached when D and A^* approach each other

to contact distances. In [13], this mechanism was shown qualitatively using the potential energy surfaces of the D-A system.

Although this model can explain the exciplex formation qualitatively, a more quantitative discussion is necessary to account for the ET processes in the exciplex. Further consideration is also necessary to clarify the relation between the Marcus model of ET and the above model. In this paper, we refine our model of exciplex formation and present some experimental results on ET in a nonpolar solvent. The relation between Marcus ET and exciplex formation is also discussed briefly.

2. MECHANISM OF ET IN NONPOLAR SOLVENT

In the case of nonpolar solvent, the solvent orientational polarization is absent, and the energies E_i and E_f of the initial (DA*) and final (D^+A^-) states of ET, respectively, do not depend on this coordinate. Except at very short distances, E_i is constant. We take $E_i = 0$ outside the contact distance. E_f is given as a function of the distance between D and A (2):

$$E_i = 0, \tag{1}$$

$$E_f = \mathrm{IP} - \mathrm{EA} - \frac{e^2}{2}\left(1 - \frac{1}{\varepsilon_{\mathrm{op}}}\right)\left(\frac{1}{a} + \frac{1}{b}\right) - \frac{e^2}{\varepsilon_{\mathrm{op}} r} \tag{2}$$

$$= E_{f\infty} - \frac{e^2}{\varepsilon_{\mathrm{op}} r}, \tag{3}$$

where IP and EA are the ionization potential of the donor and the electron affinity of the acceptor, respectively, and $\varepsilon_{\mathrm{op}}$ is the optical dielectric constant of the solvent. a and b are the radii of D and A, and r is the distance between D and A. $E_{f\infty}$ is the energy of the final state at $r = \infty$. The third term on the right-hand side of (2) gives the solvation energy of the D^+ and A^- ions. $E_{f\infty}$ can be rewritten in the following form:

$$E_{f\infty} = \Delta G^{\mathrm{AN}} + \frac{e^2}{2}\left(\frac{1}{\varepsilon_{\mathrm{op}}} - \frac{1}{\varepsilon_S^{\mathrm{AN}}}\right)\left(\frac{1}{a} + \frac{1}{b}\right), \tag{4}$$

where ΔG^{AN} and $\varepsilon_S^{\mathrm{AN}}$ are the free energy change of the reaction between D and A in AN solvent and the static dielectric constant of AN, respectively. Experimentally, it may be more convenient to use ΔG^{AN} instead of $E_{f\infty}$ because the former can be easily evaluated from the measured redox potentials of the donor and acceptor. For a pair with $a = b = 3\,\text{Å}$ in a solvent with $\varepsilon_{\mathrm{op}} = 1.88$, $E_{f\infty} = 1.65$ eV corresponds to $\Delta G^{\mathrm{AN}} = -0.85$ eV.

ET occurs when the energies of the initial and final states coincide [14, 15]. In Marcus theory, the energy coincidence occurs by the change of solvent orientational polarization, that is, the coordinate of solvent orientational polarization can be regarded as the reaction coordinate of ET reactions. This does not occur in nonpolar solvent because the solvent molecules do not have permanent dipoles. Equations (1) and (2) are plotted by broken lines in Figure 1 for a D-A pair with $E_{f\infty} = 1.65$ eV ($\varepsilon_{\mathrm{op}} = 1.88$). The two curves intersect each other at a short distance near 4.5 Å. In this case, the energy coincidence occurs by the change of intermolecular distance, and ET can occur at the intersection distance even in the absence of solvent polarization, that is, participation of solvent is not always necessary for ET to occur. This observation explains why ET can occur in nonpolar solvent. Some of the ultrafast ET that is faster than solvation may also be accounted for by the change in intermolecular distance. The coordinate of intermolecular distance can thus be regarded as another reaction coordinate of ET reactions. This point has not been stressed so far.

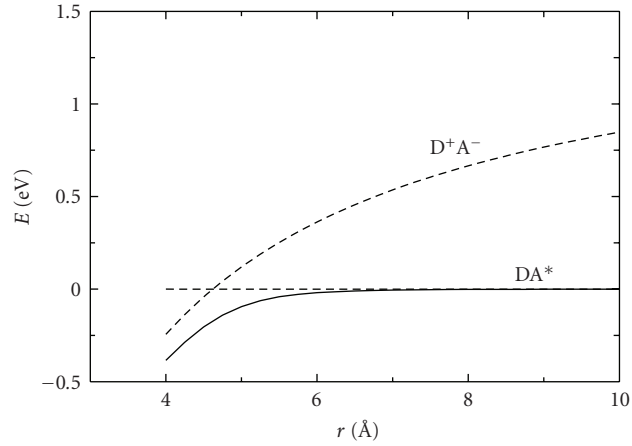

Figure 1: Potential energy curves of a D-A pair with $E_{f\infty} = 1.65$ eV ($\Delta G^{\mathrm{AN}} = -0.85$ eV) in a nonpolar solvent ($\varepsilon_S = \varepsilon_{\mathrm{op}} = 1.88$). The broken and solid curves represent the diabatic and adiabatic curves, respectively. The parameter values assumed, the molecular radii of D and A, are 3 Å, J_0 and β in (9) are 0.23 eV at 4 Å and 1 Å^{-1}, respectively. Plotting is made down to $r = 4$ Å which is smaller than $a + b = 6$ Å. This is not meaningless because D and A are often not spherical but planar and can approach to distances shorter than $a + b$.

Up to now the interactions between D and A except the Coulomb interaction have been neglected. At short distances quantum mechanical interactions between D and A become important. At such distances, the DA* and D^+A^- states are no longer pure eigenstates but are mixed with each other. The resulting state ϕ is given by

$$\phi = c_1\psi_1 + c_2\psi_2, \tag{5}$$

where ψ_1 and ψ_2 are the diabatic states. The energies $E_\pm$ of the new adiabatic states are given using the energies E_1 and E_2 of the diabatic states

$$E_\pm = \frac{E_1 + E_2}{2} \pm \frac{\sqrt{\Delta_{12}^2 + 4H_{12}^2}}{2}, \tag{6}$$

$$\Delta_{12} = |E_1 - E_2|, \tag{7}$$

$$H_{12} = \langle \psi_1 | H | \psi_2 \rangle, \tag{8}$$

where H_{12} is the electronic coupling matrix element and is assumed to decrease exponentially with distance

$$H_{12}^2 = J_0^2 \exp[-\beta(r - r_0)]. \tag{9}$$

The energy E_- calculated from (6) with $J_0 = 0.23$ eV at $r_0 = 4\,\text{Å}$ and $\beta = 1\,\text{Å}^{-1}$ is plotted by the solid curve in Figure 1.

The adiabatic state ϕ given by (5) is the exciplex state. The electronic structure of the exciplex state changes with distance. At distances longer than the intersection distance, the exciplex state is more like the DA^* state, whereas at shorter distances, it is more like the D^+A^- state. When D and A approach each other from long distances to short distances through the intersection point, the exciplex state changes from almost neutral to an ionic one. In other words, the decrease in D-A distance induces (adiabatic) ET to form the ionic exciplex. This clearly shows that even in the absence of solvent orientational polarization, ET (or exciplex formation) can occur with the change in intermolecular distance. Thus the well-known experimental results that exciplex formation is efficient in nonpolar solvent can be understood. If D and A are close to each other when A is excited, the rate of ET induced by change of r can be of the order of the frequency of intermolecular stretching vibration in the exciplex (typically $\sim 100\,\mathrm{cm}^{-1}$). The rate can be higher than that of solvent polarization, and this mechanism can explain at least some of the ultrafast ET reported so far.

When $-\Delta G^{AN}$ is larger, the initial and final states intersect each other at longer distances (Figure 2 for $E_{f\infty} = 0.9\,\mathrm{eV}$ or $\Delta G^{AN} = -1.60\,\mathrm{eV}$), and ET is expected to occur at longer distances (R_0 is the intersection distance). In this case, however, the contribution of intramolecular vibrations to ET should also be taken into account. In Figure 2, the broken curves represent the potential energy curves of the D^+A^- state with intramolecular vibrational quanta. These curves intersect the curve of the DA^* state at shorter distances. This gives rise to ET at shorter distances in addition to ET at the original distance. On the other hand, the potential energy curves of the DA^* state with vibrational quanta gives rise to ET at longer distances. According to Tachiya and Seki [16], the first-order ET rate in this case is given by

$$k(r) = \frac{2\pi}{\hbar} J_0^2 \exp\left[-\beta(r - r_0)\right] \sum_i F_i \delta\left(ih\nu + E_{f\infty} - \frac{e^2}{\varepsilon_{op} r}\right),$$
$$F_i = \exp(-s) \exp\left(\frac{ih\nu}{2k_B T}\right) I_{|i|}(z), \tag{10}$$

where β is the attenuation coefficient of ${H_{12}}^2$ with distance, $I_{|i|}(z)$ is the modified Bessel function of the first kind:

$$s = \Lambda(2n+1) \quad n = \frac{1}{\left[\exp\left\{h\nu/(k_B T)\right\} - 1\right]},$$
$$z = 2\Lambda\sqrt{n(n+1)} \quad \Lambda = \frac{\lambda}{(h\nu)}, \tag{11}$$

where λ denotes the vibrational reorganization energy. In Figure 3, $k(r)$ is plotted as a function of r for three values of $E_{f\infty}$ with $J_0 = 100\,\mathrm{cm}^{-1}$ at 6 Å, $\beta = 1\,\text{Å}^{-1}$, $\nu = 1500\,\mathrm{cm}^{-1}$, and $\lambda = 0.3\,\mathrm{eV}$. ET occurs at discrete r values, where the potential energy curves of the initial and final states intersect. The point $r = 7.7\,\text{Å}$ of the $E_{f\infty} = 1.0\,\mathrm{eV}$ curve corresponds to the distance where the initial and final state curves with zero vibrational energies intersect. $k(r)$ decreases rapidly at distances longer than this because both H_{12} and F_i (the Franck-Condon factor) decrease with increasing distance. At distances shorter than this, H_{12} increases and F_i decreases with decreasing distance, and as a result $k(r)$ first increases and then decreases slowly. For curves with $E_{f\infty} = 0.5$ and 1.72 eV, the intersection distances are 11.2 and 4.5 Å, respectively.

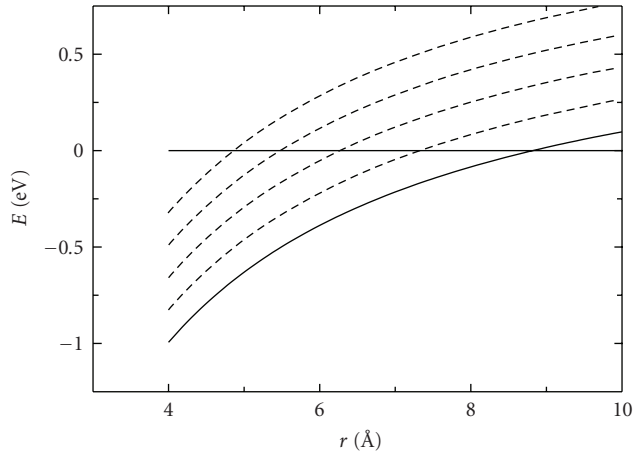

Figure 2: Potential energy curves of a D-A pair with $E_{f\infty} = 0.9\,\mathrm{eV}$ ($\Delta G^{AN} = -1.6\,\mathrm{eV}$) in a nonpolar solvent ($\varepsilon_S = 1.88$). The broken curves are the free energy curves of the final state with vibrational quanta ($\nu = 1500\,\mathrm{cm}^{-1}$).

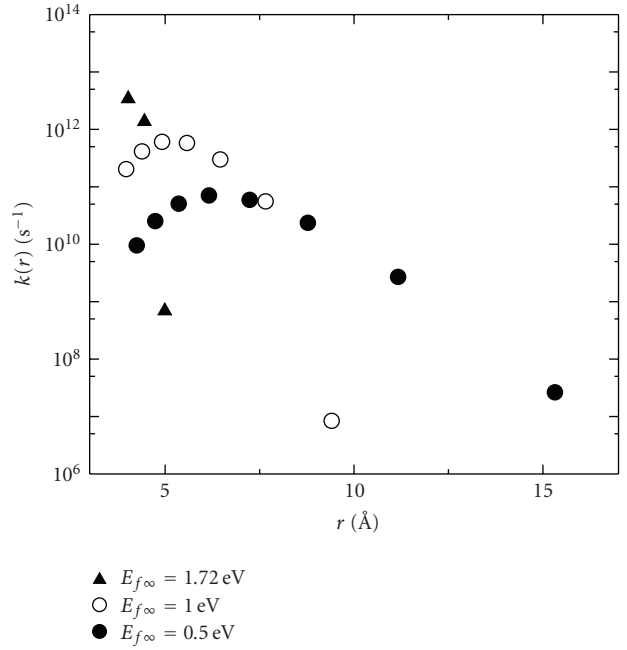

Figure 3: First-order ET rate in nonpolar solvent calculated for three values of $E_{f\infty}$ with $J_0 = 100\,\mathrm{cm}^{-1}$ at 6 Å, $\beta = 1\,\text{Å}^{-1}$, $\nu = 1500\,\mathrm{cm}^{-1}$, and $\lambda = 0.3\,\mathrm{eV}$. ET occurs at discrete r values.

3. ET REACTIONS IN POLAR SOLVENT

ET occurs when the energies of the initial and final states coincide [14, 15]. However, because the entropy does not change during ET, one can say that ET occurs when the free

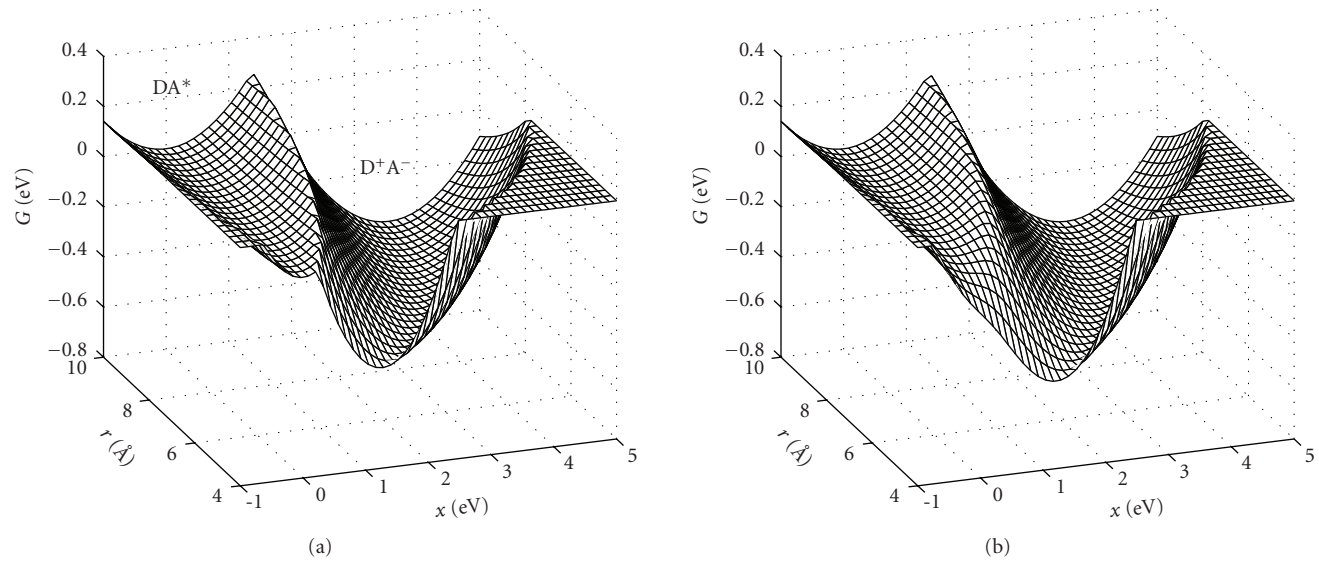

Figure 4: Free energy surfaces of a D-A pair with $\Delta G^{AN} = -0.4$ eV in AN solvent. Only the parts relevant to ET reactions are shown, (a) the mixing of the initial and final states not taken into account; (b) mixing taken into account.

energies of the initial and final states coincide. In solvents with permanent dipoles, the free energies of the initial and final states of ET are functions of both intermolecular distance r and solvent orientational polarization x. x can be given by

$$x = e\Delta V = e(V_D - V_A), \tag{12}$$

where V_D and V_A are the electrostatic potentials at the positions of D and A generated by the solvent dipoles. The free energies are given by [14, 17]

$$\begin{aligned} G_i &= \frac{1}{4\lambda}x^2, \\ G_f &= \frac{1}{4\lambda}(x - 2\lambda)^2 + \Delta G, \end{aligned} \tag{13}$$

where λ and ΔG are the reorganization energy and the free energy change of reaction, respectively, and are given by (14)

$$\begin{aligned} \lambda &= \frac{e^2}{2}\left(\frac{1}{\varepsilon_{op}} - \frac{1}{\varepsilon_S}\right)\left(\frac{1}{a} + \frac{1}{b} - \frac{2}{r}\right), \\ \Delta G &= \Delta G^{AN} + \frac{e^2}{2}\left(\frac{1}{\varepsilon_S} - \frac{1}{\varepsilon_S^{AN}}\right)\left(\frac{1}{a} + \frac{1}{b} - \frac{2}{r}\right), \end{aligned} \tag{14}$$

where ε_{op} is the optical dielectric constant of the solvent. G_i and G_f are functions of x and r, and represent 2-dimensional free energy surfaces. In this case, both x and r are regarded as reaction coordinates of ET reactions. The free energy surfaces are plotted in Figure 4(a) for a D-A pair ($\Delta G^{AN} = -0.4$ eV) in AN solvent ($\varepsilon_{op} = 1.8$ and $\varepsilon_S = 37.5$). Figure 4(b) shows the surfaces obtained by mixing the DA* and D^+A^- states corresponding to the same x and r values. In Figure 4, only the parts of the surfaces which are important for ET reactions are shown, and the surfaces in large and small x regions are artificially cut by the plane $G = 0.15$ eV so that one can see the inside of the valleys. The surfaces are smoother at shorter distances in Figure 4(b) than in Figure 4(a). This is the exciplex region, where the two states are mixed significantly. Figure 5 shows the contour plot of Figure 4(b), and some typical processes related to fluorescence quenching are also shown by arrows.

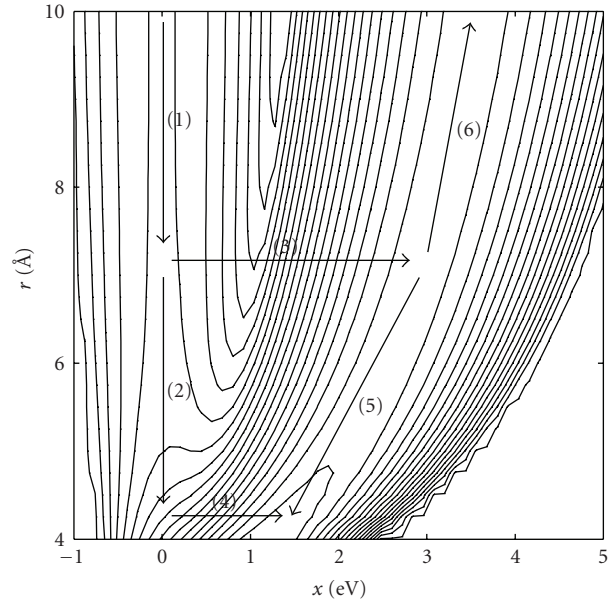

Figure 5: Contour plot of Figure 4(b). The arrows show the typical processes involved in fluorescence quenching.

From Figures 4 or 5, the relation between Marcus ET and exciplex formation is apparent. We consider a charge separation reaction. Just after excitation, the system is in the initial state DA*, and is at the bottom ($x = 0$). D and A approach each other by process (1) of Figure 5. Marcus ET

Table 1: Parameters R_0 and k_0 determined by analyzing the fluorescence decay curves.

	$E_{f\infty}$/eV	$-\Delta G^{AN}$/eV	R_0/Å	k_0/s^{-1}
C153-TMPD(0.2 M)	0.92	0.78	11.1	2.9×10^{10}
C522-TMPD(0.2 M)	0.81	0.89	12.2	3.7×10^{10}
C152-TMPD(0.2 M)	0.63	1.07	15.2	4.2×10^{8}

$E_{f\infty}$ was calculated from ΔG^{AN} using (4). $\varepsilon_S = \varepsilon_{op} = 2.16$ for liquid paraffin and $a = 3.5$ Å for TMPD and $b = 3.9$ Å for coumarins.

occurs when the system crosses the barrier that separates the initial and final states (in other words, when x changes: process (3)). The species D^+A^- generated by process (3) can either dissociate to form free ions by process (6) or form the exciplex by process (5) that involves the decrease in distance r between D^+ and A^-. The exciplex can also be formed by process (2) that occurs after process (1). Process (2) also involves the decrease in r. When r decreases, exciplex formation (charge separation) can occur even when x remains 0 (see discussion on ET in nonpolar solvent). The exciplex formed by process (2) is not in equilibrium with respect to x and can change to the equilibrated exciplex with the change in x (process (4)). This is accompanied by further charge separation within the exciplex. The rates and importances of processes (1)–(6) depend on the rate of diffusion of D and A, solvent relaxation time, interaction energy, and so forth, even for fixed ΔG^{AN}. The relative importance of Marcus ET and exciplex formation in fluorescence quenching will change with the value of ΔG^{AN}.

Some of the existing experimental results were discussed in detail elsewhere [15] on the basis of 2-dimensional free energy surfaces.

4. EXPERIMENTAL STUDY OF FLUORESCENCE QUENCHING IN NONPOLAR SOLVENT

In previous papers [9–11], we analyzed the transient effect in fluorescence quenching by ET at high quencher concentrations to determine experimentally the distance dependence of ET rates in solution. The distribution of ET distance was calculated by using the rate parameters obtained. The studies were made in polar and nonpolar solvents. In this paper, we report another study of the transient effect in a nonpolar solvent and discuss the result on the basis of the ET mechanism described in Section 2. Experimental method and data analysis have already been reported [11], and they are described briefly here.

Coumarin derivatives (C152, C153, C522; electron acceptors) were used as fluorescers and N,N,N',N'-tetramethyl-p-phenylenediamine (TMPD; electron donor) was used as quencher. The oxidation-reduction potentials of these compounds were taken from literature [18]. These values were used to calculate the free energy change ΔG^{AN} of ET reaction. Fluorescence decay curves at a quencher concentration of 0.2 M were measured by time-correlated single photon counting [9]. Fluorescence was excited using the second harmonic of a mode-locked Ti:Sa laser, and detected by an MCP-PMT. The full width at high maximum (fwhm) of the instrument response function was ~40 picoseconds. To analyze the transient effect successfully, the solvent must be highly viscous [9, 11]. We employed liquid paraffin as a viscous nonpolar solvent. Because of many restrictions (appropriate ΔG^{AN} value, high solubility in liquid paraffin, location of the absorption spectra, etc.) imposed on the D-A combinations, we could not find many D-A combinations.

The transient effect can be analyzed using the following equations [9]:

$$P(t) = \exp\left[-\frac{t}{\tau_0} - 4\pi c_0 \int_d^\infty \{1 - U(r,t)\} r^2\, dr\right], \quad (15)$$

$$\frac{\partial U(r,t)}{\partial t} = D\left(\frac{\partial^2}{\partial r^2} + \frac{2}{r}\frac{\partial}{\partial r}\right) U(r,t) - k(r)U(r,t), \quad (16)$$

where $P(t)$ is the fluorescence decay curve, $U(r,t)$ the survival probability of the D-A pair at time t that was separated by distance r when it was excited at $t = 0$. τ_0, c_0, and d are the lifetime of unquenched fluorescence, quencher concentration, and the contact distance of D and A, respectively. In obtaining (15), the initial distribution of quencher molecules is assumed to be random. D and $k(r)$ in (16) are the sum of the diffusion coefficients of D and A, and the first-order ET rate constant, respectively. Equation (16) must be solved under appropriate initial and boundary conditions. The value of D was calculated using the Stokes-Einstein equation [11].

In a previous paper [11], we analyzed the transient effect in liquid paraffin solvent, and showed that ET occurs at distances longer than the contact distances of D and A. We assumed that $k(r)$ decreases exponentially with distance

$$k(r) = A \exp[-b(r - r_0)], \quad (17)$$

where A and b are constants. From (15)–(17), we see that the shape of the fluorescence decay curve $P(t)$ is determined by the parameters A and b. Consequently, A and b can be determined by fitting the calculated decay curve (actually, its convolution with the instrument response function) to the experimental ones (it was shown that the number of parameters that can be determined by such experiment and data analysis is not more than 2) [9]. The fitting was made by a nonlinear least squares method. All the calculations were carried out numerically. Very good fittings were obtained, A and b were determined for several D-A pairs. One of the shortcomings of the use of (17) is that, if A and b corresponding to the best fit are used, $k(r)$ becomes too large at short distances. Indeed, $k(r)$ obtained from experiment exceeds 10^{15} s^{-1} for most D-A pairs at 6 Å.

In Section 2 of the present paper, we studied ET in nonpolar solvent and showed that if an intramolecular vibrational mode is taken into account, the distance dependence of $k(r)$ would be weaker when $r \leq R_0$, but $k(r)$ rapidly decrease when $r > R_0$, with R_0 being the distance where the potential energy curves of the initial and final states in the absence of intramolecular vibrational mode intersect (see Figure 3). Figure 3 shows that the dependence of $k(r)$ on r changes with $E_{f\infty}$ (or ΔG^{AN}). In Table 1 are shown the values

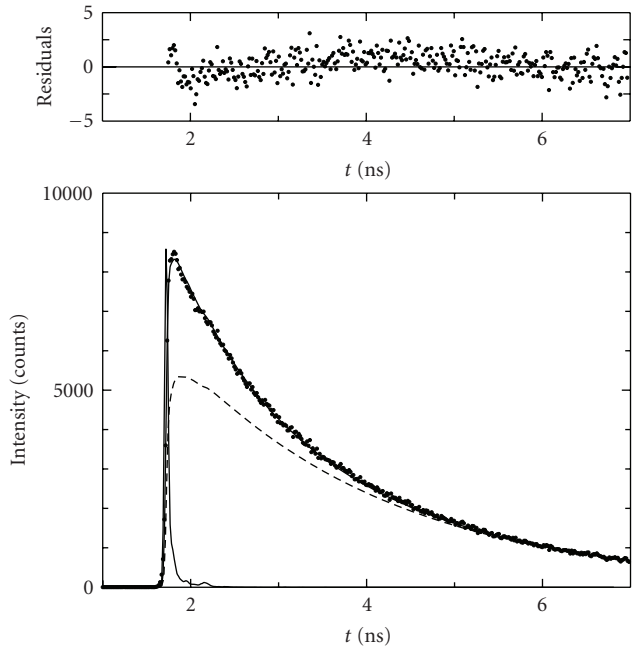

Figure 6: Observed decay curves (dots) of fluorescence of C522 quenched by TMPD (0.2 M) in liquid paraffin at 296 K, calculated best-fit to it (solid line), hypothetical decay curve (broken line), and residuals (upper dots). The thin solid line indicates the instrument response function. The ET parameters obtained are $R_0 = 12.2\,Å$ and $k_0 = 3.7 \times 10^{10}\,s^{-1}$, respectively, with $\chi^2 = 1.2786$. See the text for the hypothetical decay curve.

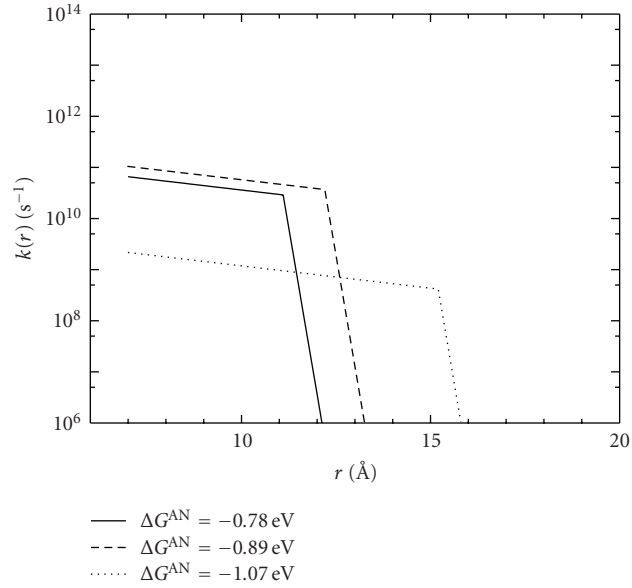

Figure 7: First-order ET rate of the three D-A pairs obtained from R_0, k_0, (18) and (19). The ΔG^{AN} values correspond to the D-A pairs given in Table 1.

of $E_{f\infty}$ and ΔG^{AN} [18] for the D-A combinations employed in this paper. These values lie in a relatively narrow range, and we can assume the same functional form for $k(r)$ for all the D-A combinations to analyze the experimental data

$$k(r) = k_0 \exp\left[-0.2(r - R_0)\right] \qquad \text{for } d < r \le R_0, \tag{18}$$

$$k(r) = k_0 \exp\left[-10(r - R_0)\right] \qquad \text{for } R_0 < r, \tag{19}$$

where d is the contact distance of D and A, and $k_0 = k(R_0)$. According to (18) and (19), inside the radius R_0, $k(r)$ decreases slowly with increasing distance, while outside this radius it decreases rapidly. If (18) and (19) are adopted, the parameters that determine the shape of the decay curve $P(t)$ are R_0 and k_0: they are determined from the fitting. The coefficient -0.2 in (18) was chosen to get better fittings.

The distribution $Y(r)$ of ET distance is given by the following equation [10]:

$$Y(r) = 4\pi r^2 c_0 k(r) \int_0^\infty q(r,t)P(t)\,dt, \tag{20}$$

where $q(r,t) = c(r,t)/c_0$ with $c(r,t)$ being the concentration profile of the quencher. $q(r,t)$ satisfies (16) with $U(r,t)$ replaced by $q(r,t)$. Consequently, $Y(r)$ can be calculated if the ET parameters R_0 and k_0 are determined. These calculations were also carried out numerically. $Y(r)dr$ gives the probability that ET occurs from the donor to the acceptor over a distance between r and $r + dr$. Integration of $Y(r)$ over r gives the quantum yield of ET reaction.

The fluorescence decay is faster for D-A pairs with higher $-\Delta G^{AN}$ values. This is also true for the decay due to ET reaction only (i.e., the decay after eliminating the monomolecular decay of the excited fluorescer). The transient effect is more pronounced for pairs with higher $-\Delta G^{AN}$ values. Figure 6 shows the experimental decay curve (dots) and the calculated best-fit one (solid curve, actually this is the convolution of the calculated curve with the instrument response function [9]) of the C522-TMPD(0.2 M) pair. Also is shown in Figure 6 a hypothetical decay curve (broken curve) that would be observed if there was no transient effect. This curve was obtained by calculating the convolution of the instrument response function with an exponential function with the same decay time as that in the longer time region of the observed decay. The difference between the observed and hypothetical decay curves found in the shorter-time region is due to the transient effect that we analyze. The fit of the calculated decay curve with the observed one is satisfactory, that is, the transient effect is reproduced well by the analysis. The parameters R_0 and k_0 corresponding to the best fit were $12.2\,Å$ and $3.7 \times 10^{10}\,s^{-1}$, respectively. The fit for C152-TMPD pair is not as good as for C522-TMPD pair. This might be because $k(r)$ of the same functional form, in particular, the slope in the longer distance range, has been used. However, if functions with smaller slopes are used, the fitting calculation becomes unstable and it does not give reasonable results. So we did not change the functional form of $k(r)$ for different D-A pairs. The parameters obtained from experiment are summarized in Table 1. The stronger transient effect found experimentally for D-A pairs with higher $-\Delta G^{AN}$ values is reflected on the larger R_0 values of these pairs. Figure 7 shows the distance dependence of $k(r)$

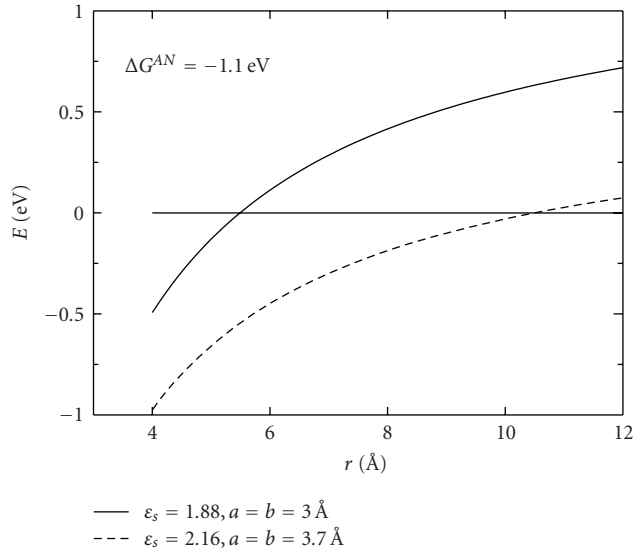

Figure 8: Free energy curves of a D-A pair with $\Delta G^{AN} = -1.1$ eV in a nonpolar solvent. Curves for pairs with different molecular radii and in different solvents are compared.

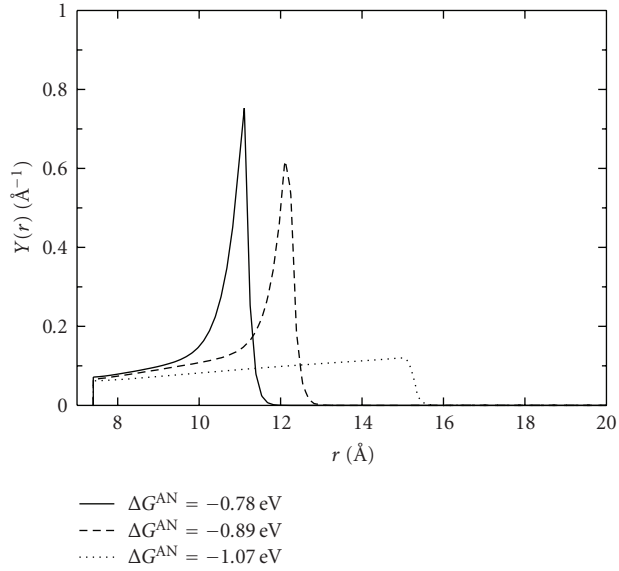

Figure 9: Distribution of ET distance at a quencher concentration of 0.2 M calculated from (20) using R_0 and k_0 determined experimentally.

obtained using R_0 and k_0. The largest value of $k(r)$ obtained is $\sim 1 \times 10^{11}$ s^{-1} in the whole range of r: we have obtained good fits with reasonable values of $k(r)$.

It is clear from Table 1 that R_0 increases with increasing $-\Delta G^{AN}$ of the D-A pair. This is expected from the model already described in Section 2. The same model predicts that k_0 decreases with increasing R_0. The experimental result seems to be consistent with this, although k_0 of the C522-TMPD pair ($R_0 = 12.2$ Å) is slightly larger than that of the C153-TMPD pair ($R_0 = 11.1$ Å). Thus the experiment and the prediction from the model are in qualitative agreement.

R_0 is the distance where the free energy curves in the absence of intramolecular vibrational mode intersect each other, and it can readily be obtained from (1) and (3). Figure 8 shows the potential energy curves for a D-A pair with $\Delta G^{AN} = -1.1$ eV (corresponding to the C152-TMPD pair). The solid E_f curve gives $R_0 \sim 5.5$ Å, which is much smaller compared with that (15.2 Å) experimentally found for C152-TMPD pair. For this case, however, the parameter values ($a = b = 3$ Å, $\varepsilon_S = 1.88$) used so far are not appropriate. More realistic values are $a = 3.9$ Å (for coumarins), $b = 3.5$ Å (for TMPD) (both calculated empirically [19, 20]), and $\varepsilon_S = 2.16$. The broken E_f curve using these parameters gives R_0 ($\sim$10.5 Å) that is much larger than the previous one and closer to the experiment. The agreement, however, is not quantitative. The disagreement may be caused by insufficient accuracy of the calculation of potential energy surfaces, and also by possible nonrandom distribution of quencher molecules in liquid paraffin solvent that consists of large molecules compared to solute molecules. These are problems to be solved in the future.

Figure 9 shows the distribution of ET distance at $c_0 = 0.2$ M calculated from (20). ET occurs at distances longer than the contact distance of D and A, as has been reported in a previous paper [10, 11]. We see from Figure 9 that each $Y(r)$ curve has a maximum at distance R_0, in spite of the assumption that $k(r)$ increases with decreasing r. This can be understood as follows [10]. Before excitation, the distribution of D and A is random (or uniform). After excitation, the reaction first occurs between D and A with initial intermolecular distances smaller than R_0. This is because the solvent is highly viscous and D and A cannot approach quickly by diffusion. This results in a decrease in the concentration of D-A pairs with $r < R_0$, and in the time following, other D and A can approach by diffusion to the $r < R_0$ region. Because $k(r)$ suddenly increases to a high value at $r = R_0$ (except for C152-TMPD pair), the reaction occurs efficiently near this point yielding a large value of $Y(r)$ near $r = R_0$, and only a small fraction of D-A pairs is left for further approach. In the case of C152-TMPD, because $k(r)$ is not large enough in $r < R_0$, the reaction at R_0 is not very efficient and a larger fraction of D-A pairs can reach the $r < R_0$ region to react there.

Figure 7 indicates that $k(r)$ of the C522-TMPD pair ($\Delta G^{AN} = -0.89$ eV, pair 1) is larger than that of the C153-TMPD pair ($\Delta G^{AN} = -0.78$ eV, pair 2) at any value of r. However, the maximum value of $Y(r)$ of pair 1 is smaller than that of pair 2. This can be interpreted in the following way. Because R_0 and $k(r)$ of pair 1 are larger than those of pair 2, the reaction of pair 1 just after excitation is more efficient than that of pair 2. This implies that a smaller number of pairs is available for reaction near $r = R_0$ in the time following. These features can explain why the maximum value of $Y(r)$ of pair 1 is smaller than that of pair 2. The quantum yield of ET reaction is 0.74, 0.81, and 0.73 for C153-TMPD, C522-TMPD, and C152-TMPD pairs, respectively, at $c_0 = 0.2$ M.

5. CONCLUDING REMARKS

In nonpolar solvents, where solvent orientational polarization is absent, ET can occur by the change in intermolecular D-A distance. Efficient exciplex formation in nonpolar solvents, a well-known experimental result, can thus be understood. Intermolecular distance can be regarded as the reaction coordinate of ET reactions. In polar solvents, the free energies are functions of both intermolecular distance and solvent orientational polarization. The relation between Marcus ET and exciplex formation was discussed on the basis of 2-dimensional free energy surfaces. Some experimental results were presented on the transient effect in fluorescence quenching in a nonpolar solvent. The results were analyzed by assuming a distance dependence of the ET rate that is consistent with the above model.

REFERENCES

[1] H. Leonhardt and A. Weller, "Elektronenübertragungsreaktionen des angeregten Perylens," *Berichte der Bunsen-Gesellschaft für Physikalische Chemie*, vol. 67, no. 8, pp. 791–795, 1963.

[2] M. Gordon and W. R. Ware, Eds., *The Exciplex*, Academic Press, New York, NY, USA, 1975.

[3] H. Beens and A. Weller, "Excited molecular z-complexes in solution," in *Organic Molecular Photophysics*, J. B. Birks, Ed., vol. 2, pp. 159–215, John Wiley & Sons, New York, NY, USA, 1975.

[4] N. Mataga, "Photochemical charge transfer phenomena-picosecond laser photolysis studies," *Pure and Applied Chemistry*, vol. 56, no. 9, pp. 1255–1268, 1984.

[5] I. R. Gould, R. H. Young, L. J. Mueller, and S. Farid, "Mechanisms of exciplex formation. Roles of superexchange, solvent polarity, and driving force for electron transfer," *Journal of the American Chemical Society*, vol. 116, no. 18, pp. 8176–8187, 1994.

[6] I. R. Gould, R. H. Young, L. J. Mueller, A. C. Albrecht, and S. Farid, "Electronic structures of exciplexes and excited charge-transfer complexes," *Journal of the American Chemical Society*, vol. 116, no. 18, pp. 8188–8199, 1994.

[7] Y. L. Chow and C. I. Johansson, "Exciplexes of (dibenzoylmethanato)boron/benzenes: the control of exciplex electronic structure," *The Journal of Physical Chemistry*, vol. 99, no. 49, pp. 17558–17565, 1995.

[8] K. N. Grzeskowiak, S. E. Ankner-Mylon, S. N. Smirnov, and C. L. Braun, "Exciplex dipole moments: excited cyanoanthracenes in neat methylbenzene solvents," *Chemical Physics Letters*, vol. 257, no. 1-2, pp. 89–92, 1996.

[9] S. Murata, S. Y. Matsuzaki, and M. Tachiya, "Transient effect in fluorescence quenching by electron transfer. 2. Determination of the rate parameters involved in the Marcus equation," *The Journal of Physical Chemistry*, vol. 99, no. 15, pp. 5354–5358, 1995.

[10] S. Murata and M. Tachiya, "Transient effect in fluorescence quenching by electron transfer. 3. Distribution of electron transfer distance in liquid and solid solutions," *The Journal of Physical Chemistry*, vol. 100, no. 10, pp. 4064–4070, 1996.

[11] L. Burel, M. Mostafavi, S. Murata, and M. Tachiya, "Transient effect in fluorescence quenching by electron transfer. 4. Long-range electron transfer in a nonpolar solvent," *The Journal of Physical Chemistry A*, vol. 103, no. 30, pp. 5882–5888, 1999.

[12] S. Iwai, S. Murata, and M. Tachiya, "Ultrafast fluorescence quenching by electron transfer and fluorescence from the second excited state of a charge transfer complex as studied by femtosecond up-conversion spectroscopy," *The Journal of Chemical Physics*, vol. 109, no. 14, pp. 5963–5970, 1998.

[13] S. Iwai, S. Murata, R. Katoh, M. Tachiya, K. Kikuchi, and Y. Takahashi, "Ultrafast charge separation and exciplex formation induced by strong interaction between electron donor and acceptor at short distances," *The Journal of Chemical Physics*, vol. 112, no. 16, pp. 7111–7117, 2000.

[14] M. Tachiya, "Generalization of the Marcus equation for the electron-transfer rate," *The Journal of Physical Chemistry*, vol. 97, no. 22, pp. 5911–5916, 1993.

[15] S. Murata and M. Tachiya, "Unified interpretation of exciplex formation and Marcus electron transfer on the basis of two-dimensional free energy surfaces," *The Journal of Physical Chemistry A*, vol. 111, no. 38, pp. 9240–9248, 2007.

[16] M. Tachiya and K. Seki, "Energy gap law of electron transfer in nonpolar solvents," *The Journal of Physical Chemistry A*, vol. 111, no. 38, pp. 9553–9559, 2007.

[17] M. Tachiya and S. Murata, "Non-Marcus energy gap dependence of back electron transfer in contact ion pairs," *Journal of the American Chemical Society*, vol. 116, no. 6, pp. 2434–2436, 1994.

[18] H. Shirota, H. Pal, K. Tominaga, and K. Yoshihara, "Substituent effect and deuterium isotope effect of ultrafast intermolecular electron transfer: coumarin in electron-donating solvent," *The Journal of Physical Chemistry A*, vol. 102, no. 18, pp. 3089–3102, 2000.

[19] J. T. Edward, "Molecular volumes and the Stokes-Einstein equation," *Journal of Chemical Education*, vol. 47, no. 4, pp. 261–270, 1970.

[20] A. Bondi, "Van der Waals volumes and radii," *The Journal of Physical Chemistry*, vol. 68, no. 3, pp. 441–451, 1964.